

3D INTENSE BEAM DYNAMICS SIMULATION BY USING MOMENTS METHOD

N. Kazarinov¹, V. Aleksandrov, V. Shevtsov

Joint Institute for Nuclear Research, Dubna

The program of the 3D intense beam dynamic simulation based on the moments method is presented.

Представлена программа трехмерного моделирования динамики интенсивных пучков, основанная на методе моментов.

PACS: 29.27.-a

INTRODUCTION

Within the framework of the Multi-Component Ion Beam code (MCIB04) [1], the program for 3D simulation of the intense charged-particle beam dynamics is created.

Fast analysis and study of the averaged beam characteristics, such as root-mean-square (RMS) dimensions, are performed by the moments method [2].

The main advantage of the moments method in comparison with macroparticle one is fast calculation and therefore applicability for transport line optimization.

The model describing the charge density of the bunched beam is introduced. The external electromagnetic fields are assumed to be linear. The approach of effective linearization [2] of both longitudinal and transversal beam self-fields gives possibility to get the closed system of the equations for second-order moments.

The fitting procedure based on minimization of a quadratic functional at any point of the beam line by using either gradient or simplex method is available [3].

BEAM MODEL

Let us consider the train of bunches (Fig. 1), moving with average velocity $\beta_0 c$ with distance between its centers of mass $\lambda = \beta_0 \lambda_0$. Here λ_0 is cyclotron RF field wavelength.

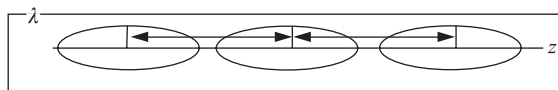


Fig. 1

¹E-mail: nyk@lnr.jinr.ru

The beam density may be defined as

$$\rho(x, y, z - \beta_0 ct) = N \rho_{\parallel}(z - \beta_0 ct) \rho_{\perp}(x, y), \quad (1)$$

where $N = \frac{I\lambda}{Ze\beta_0 c}$ — the number of particles at spatial period λ ; I — beam current; Ze — ion charge.

Longitudinal ρ_{\parallel} and transverse ρ_{\perp} densities are equal to

$$\rho_{\parallel}(z) = \frac{1}{\sqrt{2\pi}\sigma_z} \sum_{n=-\infty}^{\infty} \exp\left(-\frac{(z - n\lambda)^2}{2\sigma_z^2}\right), \quad (2a)$$

$$\rho_{\perp}(x, y) = \frac{1}{2\pi\sigma_x\sigma_y} \exp\left(-\frac{x^2}{2\sigma_x^2} - \frac{y^2}{2\sigma_y^2}\right). \quad (2b)$$

According to formula (2a), longitudinal density is periodical function $\rho_{\parallel}(z) = \rho_{\parallel}(z + \lambda)$ with a constant number of particles at period λ :

$$\int_{-\lambda/2}^{\lambda/2} \rho_{\parallel}(z) dz = N. \quad (3)$$

In the case $\sigma_z \gtrsim \lambda$ this model describes the beam with constant density and for $\sigma_z \ll \lambda$ gives Gaussian beam. The z -dependencies of the longitudinal beam density for various values of ratio λ/σ_z are shown in Fig. 2.

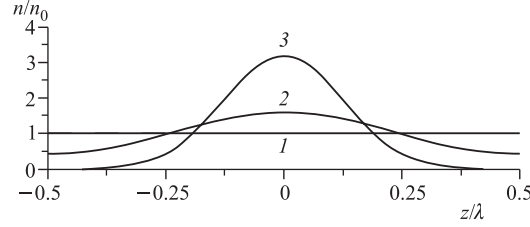


Fig. 1. Longitudinal beam density. 1 — $\lambda/\sigma_z = 1$; 2 — $\lambda/\sigma_z = 4$; 3 — $\lambda/\sigma_z = 8$

BEAM SELF-FIELD

By using formulae (1) and (2) the beam self-field may be represented as follows [4]:

$$\begin{aligned} E_x &\cong 2\pi ZeN \rho_{\parallel}(z - \beta_0 ct) \sigma_x \sigma_y \int_0^{\infty} \frac{x}{(\sigma_x^2 + s)R(s)} \rho_{\perp}(T) ds, \\ E_y &\cong 2\pi ZeN \rho_{\parallel}(z - \beta_0 ct) \sigma_x \sigma_y \int_0^{\infty} \frac{y}{(\sigma_y^2 + s)R(s)} \rho_{\perp}(T) ds, \\ T &= \frac{x^2}{\sigma_x^2 + s} + \frac{y^2}{\sigma_y^2 + s}; \quad R(s) = \sqrt{(\sigma_x^2 + s)(\sigma_y^2 + s)}, \\ E_z &\cong 2ZeN \rho'_{\parallel}(z - \beta_0 ct) \left(\ln \frac{b}{a} + \frac{1}{2} - \frac{x^2 + y^2}{2a^2} \right), \quad x^2 + y^2 \leq a^2. \end{aligned} \quad (4)$$

Here $a = \sqrt{2(\sigma_x^2 + \sigma_y^2)}$ — RMS radius of the beam; b — vacuum pipe radius, and prime denotes derivative with respect to z .

MOMENTS EQUATIONS

Let us define the second-order moments M of the beam distribution function f :

$$M = \overline{YY^T} = \frac{1}{N} \int YY^T f dy, \quad (5)$$

where superscript T denotes transpose vector or matrix, $Y^T = (x, y, x', y', z - \beta_0 ct, \delta) = (X^T, V^T, Y_{\parallel}^T) = (Y_{\perp}^T, Y_{\parallel}^T)$ — vector of phase space coordinates of the particle; $\delta = (\beta - \beta_0)/\beta_0$ — relative momentum spread. Integration in (4) is fulfilled over all the phase space occupied by bunch particles (at one spatial period), prime denotes derivative with respect to longitudinal coordinate of the bunch center of mass.

The equations for transverse second-order moments $M_{\perp} = \overline{Y_{\perp} Y_{\perp}^T}$ do not change significantly in comparison with the case of non-bunched beam [2]:

$$M'_{\perp} = AM_{\perp} + M_{\perp}A^T; \quad A = \begin{pmatrix} 0 & E \\ b_{\text{ext}} + b_s & a_{\text{ext}} \end{pmatrix}. \quad (6)$$

Here M_{\perp} , A are fourth-order matrices; E is second-order unit matrix; a_{ext} and b_{ext} are 2×2 matrices defined by external fields. Second-order matrix b_s depends on RMS dimensions and is defined by beam self-fields:

$$b_s = k_{\perp} \frac{Z}{A} \frac{I}{I_A} \frac{1}{\beta_0^3} \frac{1}{\sigma_x + \sigma_y} \begin{pmatrix} 1/\sigma_x & 0 \\ 0 & 1/\sigma_y \end{pmatrix}, \quad (7)$$

where A — ion mass; $I_A = mc^3/e$ — Alfven's current.

The bunching factor k_{\perp} is connected with changing of the transverse beam self-fields due to changing of the longitudinal density:

$$k_{\perp} = \lambda \int_{-\lambda/2}^{\lambda/2} \rho_{\parallel}^2(z) dz = \sqrt{\frac{\overline{z^2}}{z_0^2}} F_{\perp} \left(\frac{\overline{z^2}}{z_0^2} \right). \quad (8)$$

Here $\sqrt{\overline{z^2}}$ is current longitudinal RMS dimension of the bunch:

$$\overline{z^2} = \int_{-\lambda/2}^{\lambda/2} z^2 \rho_{\parallel}(z) dz \quad (9)$$

and $\sqrt{\overline{z^2}} = \lambda/\sqrt{3}$ its value for non-bunched beam. The plot of function $F_{\perp}(x)$ is shown in Fig. 3, *a*.

As can be seen from Fig. 3, *a*, function $F_{\perp}(x)$ is approximately equal to unity with difference not greater than 6%. In the program this function is represented as the sixth-order polynomial.

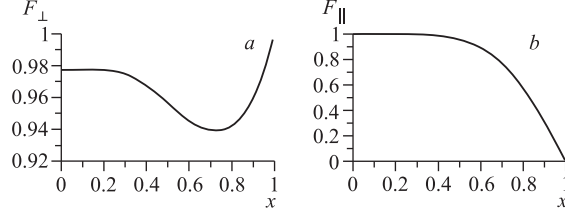


Fig. 2.

The equations for the longitudinal second-order moments M_{\parallel} have the form

$$M_{\parallel} = \overline{Y_{\parallel} Y_{\parallel}^T} = \begin{pmatrix} \overline{z^2} & \overline{z\delta} \\ \overline{z\delta} & \overline{\delta^2} \end{pmatrix}, \quad (10a)$$

$$\left(\overline{z^2}\right)' = 2 \overline{z\delta}, \quad (10b)$$

$$\left(\overline{z\delta}\right)' = \overline{\delta^2} + \frac{Ze}{Am\beta_0^2 c^2} \overline{zE_z}, \quad (10c)$$

$$\left(\overline{\delta^2}\right)' = \frac{Ze}{Am\beta_0^2 c^2} \frac{\overline{zE_z}}{z^2} \overline{z\delta}. \quad (10d)$$

Computation of average $\overline{zE_z}$ in accordance with formulae (4) and (5) results in

$$\frac{Ze}{Am\beta_0^2 c^2} \overline{zE_z} = k_{\parallel} \frac{Z}{A} \frac{I}{I_A} \frac{1}{\beta_0^3} \left(\ln \frac{b}{\sqrt{2(\sigma_x^2 + \sigma_y^2)}} + \frac{1}{4} \right). \quad (11)$$

The bunching factor of the longitudinal motion k_{\parallel} is defined by the formula

$$k_{\parallel} = \lambda \int_{-\lambda/2}^{\lambda/2} \left[\rho_{\parallel}^2(z) - \rho_{\parallel}^2\left(\frac{\lambda}{2}\right) \right] dz = k_{\perp} F_{\parallel} \left(\frac{\overline{z^2}}{z_0^2} \right). \quad (12)$$

The plot of function $F_{\parallel}(x)$ is shown in Fig. 3, *b*. In the case $x \sim 1$ function F_{\parallel} is close to zero because the longitudinal electric field of non-bunched beam is equal to zero. For the well-bunched beam ($x \ll 1$) due to small longitudinal density at point $z = \lambda/2$, formulae (11) and (12) become identical and function F_{\parallel} is close to unity. In the program, function $F_{\parallel}(x)$ is approximated by the fifth-order polynomial for all values of x .

MCIB04 CODE MODIFICATION

The 3D moments equations were introduced into existing program library code MCIB04 [1]. The interface of the program is shown in Fig. 4.

Before launching of the program the files containing the beam-line lattice, initial beam parameters and (optionally) the longitudinal magnetic field distribution have to be created.

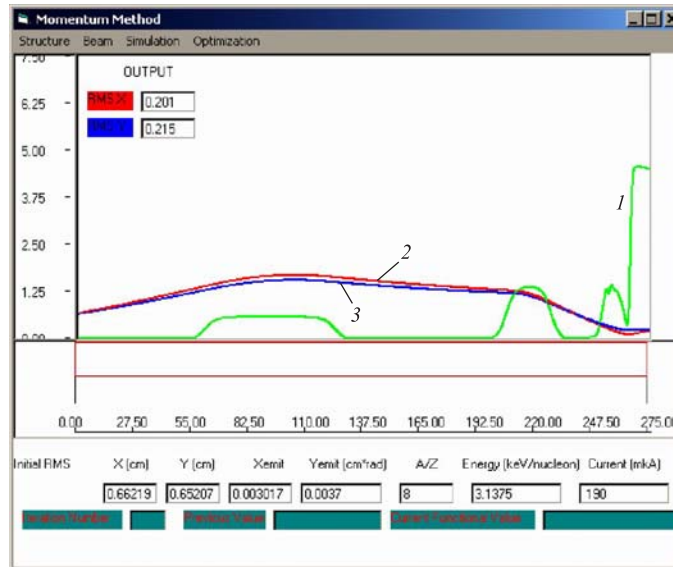


Fig. 3. Interface of the program

During operation of the program the changes of the second-order moments along the beam line are computed. The plots of the longitudinal magnetic field distribution (line 1 in Fig. 4) and RMS dimensions of the beam (line 2 — x and line 3 — y) are given at monitor. The special windows are intended for values of the beam RMS dimensions at the exit of the channel (RMSX, RMSY) and initial parameters: RMS dimensions (X , Y), emittances (X_{emit} , Y_{emit}), mass-to-charge ratio (A/Z), kinetic energy (Energy), and beam current (Current).

The fitting procedure based on minimization by using either gradient or simplex method of a quadratic functional computed for every second-order moments at any point of the beam line is available [3].

The dependencies on distance along the channel of the beam envelopes, emittances, momentum spread and other parameters are written to the file and processed by the graphing program package.

BUNCHING SYSTEM COMPUTATION

The simulation of the bunching system of the DC350 cyclotron axial injection beam line [5] was fulfilled by using created 3D version of MCIB04 code.

The bunching system consists of linear and sinusoidal bunchers. The linear buncher is placed at 275 cm and sinusoidal — at 80 cm from the median plane of the cyclotron. In the simulation all bunchers were replaced by infinitesimal width gap with variable voltage.

⁴⁸Ca beam initial parameters

Injected beam	⁴⁸ Ca ⁶⁺
Mass A	48
Charge Z	2–8
Injected current, μA	0–190
Ca beam current, μA	0–700
He beam current, μA	200
⁴⁸ Ca ⁶⁺ kinetic energy, keV/u	3.1375
Diameter, mm	8
Emittance, π mm·mrad	142

The initial parameters of the beam are listed in table.

The initial conditions for the moments were defined at the entrance of the linear buncher and were found by macroparticle simulation. Charge state distributions for ion beam and its self-fields were taken into account in this simulation.

The beam focusing is provided by two solenoids. The longitudinal magnetic field of the cyclotron is also considered.

The matching condition at the entrance of the spiral inflector corresponds to the steady state of the beam (without envelopes oscillation) in the uniform magnetic field with magnitude to be equal to the field in the cyclotron center. The amplitude

of the voltage at linear buncher was found to provide the equality $k_{\perp} = 2$ at the entrance of sinusoidal buncher.

The beam envelopes near spiral inflector of the cyclotron are shown in Fig. 5.

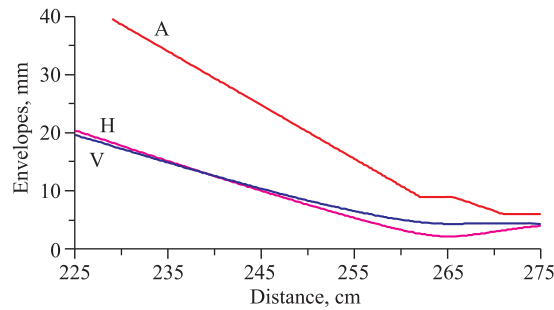


Fig. 4. Aperture (A), horizontal (H) and vertical (V) ⁴⁸Ca⁶⁺ beam envelopes near inflector

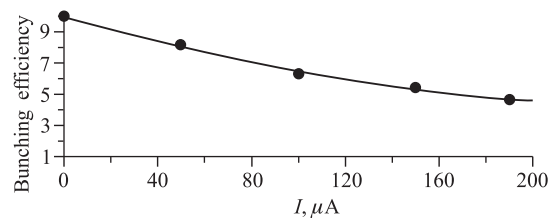


Fig. 5. Bunching efficiency versus beam current

Let us define the bunching efficiency as ratio of the number of particles within RF phase interval $|\Delta\varphi| \leq 15^\circ$ to non-bunched beam one. This quantity shows a possible increase of the number of particles captured into acceleration in the cyclotron due to the bunching system. The dependence of the bunching efficiency on the ⁴⁸Ca⁶⁺ beam current is shown in Fig. 6.

REFERENCES

1. *Aleksandrov V., Kazarinov N., Shevtsov V.* Multi-Component Ion Beam Code — MCIB04 // Proc. of XIX Rus. Particle Accelerator Conf. (RuPAC-2004), Dubna, 2004. P. 201.
2. *Kazarinov N. Yu., Perelstein E. A., Shevtsov V. F.* Moments Method in Charged Particle Beams Dynamics // Part. Accel. 1980. V. 10. P. 33–48.
3. *Kazarinov N. Yu., Shevtsov V. F.* Optimization of Transportation Channel Parameters for Beam with Big Spatial Charge. JINR Commun. P9-2002-148. Dubna, 2002.
4. *Chao A. W.* Physics of Collective Beam Instabilities in High Energy Accelerators. Wiley Series in Beam Phys. and Accelerator Technol. N. Y., 1993.
5. *Gulbekyan G. et al.* Axial Injection Channel of the DC-350 Cyclotron // Presented at 18th Intern. Conf. on Cyclotrons and Their Application, Giardini Naxos, Italy, Sept. 30–Oct. 5, 2007.